CONEM 2010
VI Congresso Nacional de Engenharia Mecânica

ABCM — COMPROMETIDA COM A PROMOÇÃO DO DESENVOLVIMENTO DA ENGENHARIA E DAS CIÊNCIAS MECÂNICAS
ASSOCIAÇÃO BRASILEIRA DE ENGENHARIA E CIÊNCIAS MECÂNICAS

VI CONGRESSO NACIONAL DE ENGENHARIA MECÂNICA
VI NATIONAL CONGRESS OF MECHANICAL ENGINEERING
18 a 21 de agosto de 2010 – Campina Grande – Paraíba - Brasil
August 18 – 21, 2010 – Campina Grande – Paraíba – Brazil

ANALYTIC BI-MATERIAL MODEL OF HUMAN LONG BONES

Paulo Pedro Kenedi, pkenedi@cefet-rj.br[1]
Ivan Ivanovitsch Thesi Riagusoff, ivanthesi@yahoo.com.br[1,2]

[1] CEFET/RJ - PPEMM - Programa de Pós-Graduação em Engenharia Mecânica e Tecnologia de Materiais
Av. Maracanã, 229, 20271-110 - Rio de Janeiro - RJ – Brazil
[2] ESSS – Rua Lauro Muller, 116 - 14º andar – 1404 – 22290-160 – Rio de Janeiro – RJ - Brazil

Abstract*. An analytic bi-material model, composed of two bone tissues, is proposed. An elliptic cross section is used to model a real medial cross section of a long bone: an external elliptic constant thickness wall is used to model the cortical tissue and an internal ellipse is used to model trabecular tissue. The objective of the analytic model is to establish an explicit relationship between applied loads and mechanical stresses generated at external surface of a medial cross section of a long bone.*

Keywords: *long bones, stress analysis, analytic model*

1. INTRODUCTION

The first works in this subject done by the authors as in (Kenedi, 2008, 2007a, 2007b), also based in (Doblaré, 2004) and (Keyak, 2000), establishes the basis of this research in bone analytic models, using mechanics of solids to estimated stresses at external surface of circular medial cross section bone. With the development of research as shown in (Kenedi, 2009a, 2009b), the bone cross section was improved to an elliptic one. In these former works only cortical tissue was recognized. In this work the trabecular bone tissue is also recognized, generating a bi-material model. Several limiting hypotheses have to be made in order to assure viability of the proposed model. For instance, cortical and trabecular bones, are supposed to be homogenous and isotropic. Loading conditions are static. Restrains are positioned only at extremities of long bones, no side ligaments or muscles are recognized. The stress analysis is made at medial cross section, therefore far from long bone ends. To maintain straightforward application of model the mathematical manipulations are kept at an introductory level, as well as, the utilization of theory of mechanics of solids.

2. ANALYTIC MODEL

The analytic model is generated through the implementation of a stress analysis of a filled elliptic medial cross section of constant thickness wall long bone. Although mechanics of solids was used only at an introductory level, the cross section geometry of the two materials elliptic model (cortical and trabecular bones) generates a relatively complex set of expressions, therefore is recommended the utilization of a mathematical software, like MathCad.

Two types of bone tissue, cortical and trabecular, were implemented considering its longitudinal mechanical properties (Rapoff, 2007) and (Turner, 1999). It is supposed that loading were divided between both types of bones, configuring a parallel arrangement, making the estimation of axial, bending, torsional and transverse shear stresses, as will be shown at section 2.2, a function of several mechanical proprieties ratios. These stress evaluations can be combined, at a given point of external surface of long bone medial cross section, to generate principal stresses and maximum shear stresses, which are key variables to any failure criteria.

Especial attention was given to maintain the analytic model expression as simple as they could be. Instead of generating few very complex expressions it was preferred generate a set of more simple expressions that are substituted in each governing expressions. This approach has many advantages, as each variable is explicitly shown, the correctness of each expression can be readily accessed and upgrades of expressions can be readily done.

Although this analytic model covers only a specific case and it is necessary the utilization of mathematical software to do the calculations, this approach is far more economical that ones uses by a traditional approach using the finite element software.

2.1 – Loading at cross section

Figure 1 shows an example of human femur hypothetical cut at a generic medial section. At a distance ***d*** away from the centre of the generic medial cross section, a static force ***P*** is applied at femur's head.

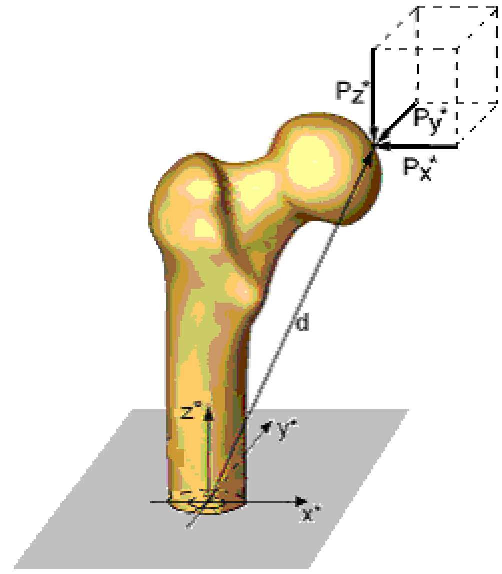

Figure 1. An example of a static load of a human femur's head.

The static force ***P*** and distance ***d*** are represented by its components in global coordinates system:

$$\boldsymbol{P} = P_x^*\vec{i} + P_y^*\vec{j} + P_z^*\vec{k} \quad \text{and} \quad \boldsymbol{d} = d_x\vec{i} + d_y\vec{j} + d_z\vec{k} \tag{1}$$

At the chosen cross section, the components of force and moments in global coordinates are:

$$\begin{pmatrix} V_x^* \\ V_y^* \\ V_z^* \end{pmatrix} = \begin{pmatrix} P_x^* \\ P_y^* \\ P_z^* \end{pmatrix} \quad \text{and} \quad \begin{pmatrix} M_x^* \\ M_y^* \\ M_z^* \end{pmatrix} = \begin{pmatrix} d_y P_z^* - d_z P_y^* \\ d_z P_x^* - d_x P_z^* \\ d_x P_y^* - d_y P_x^* \end{pmatrix} \tag{2}$$

The variables presented in bold are vectors, the components of vectors that have an asterisk are referenced to global system of coordinates. N is the axial force, V is the shear force, M is the bending moment and T is the torsional moment. $\vec{i}$, $\vec{j}$ and $\vec{k}$ are unit vectors. Note that $V_z^* = N$ and $M_z^* = T$.

2.2 - The expressions of bi-material elliptic model

Former works estimates the distribution of stresses at external surface of a medial hollow elliptic cross section of a long bone (Kenedi, 2009b, 2009a). This model uses a bi-material filled elliptic cross section, taking in account two distinct materials: trabecular and cortical bones. Figure 2, shows the geometry and the coordinate systems of this model.

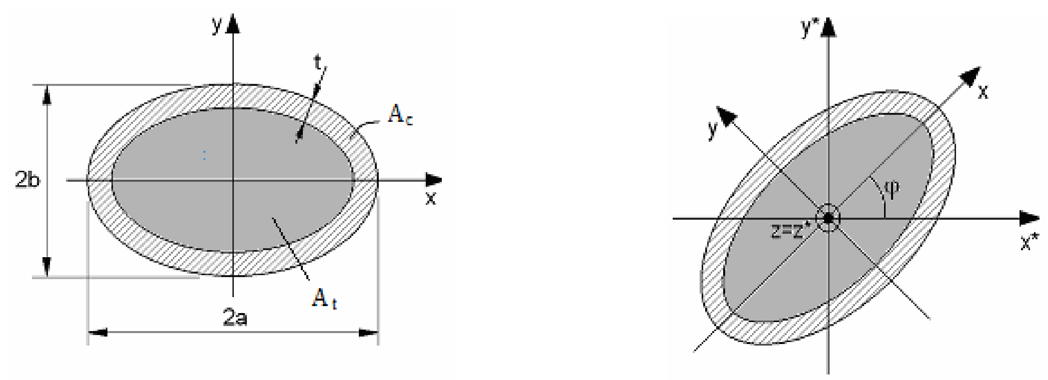

Figure 2. (a) Idealized bi-material elliptic cross section and (b) local and global coordinate systems.

Figure 2.a shows a bi-material filled elliptic cross section, with constant thickness wall *t*, with long axis *2a* and short axis 2*b*, and cross sectional areas A_c and A_t, respectively cortical and trabecular bone areas. Fig. 2.b shows two coordinates systems: local and global. The local coordinates (x,y,z) are attached to cross section, where *x* and *y* axis are respectively, coincident with *2a* and *2b* axis. The *z* axis is obtained by the application of the *right-hand rule*. Each cross section has its own local axis configuration, always maintaining *x* axis coincident with *2a*. Global coordinates (x^*,y^*,z^*) has always the same orientation in space, where x^*y^* is a horizontal plane, x^*z^* and y^*z^* are vertical planes. φ is the angle between coordinate systems.

The force and moments components, written in local coordinates, are:

$$\begin{pmatrix} V_x \\ V_y \\ V_z \end{pmatrix} = \begin{pmatrix} P_x^* \cos(\varphi) + P_y^* \sin(\varphi) \\ -P_x^* \sin(\varphi) + P_y^* \cos(\varphi) \\ P_z^* \end{pmatrix} \quad \text{and} \quad \begin{pmatrix} M_x \\ M_y \\ M_z \end{pmatrix} = \begin{pmatrix} M_x^* \cos(\varphi) + M_y^* \sin(\varphi) \\ -M_x^* \sin(\varphi) + M_y^* \cos(\varphi) \\ M_z^* \end{pmatrix} \tag{3}$$

Figure 3 shows all the loads acting at a medial cross section of a long bone.

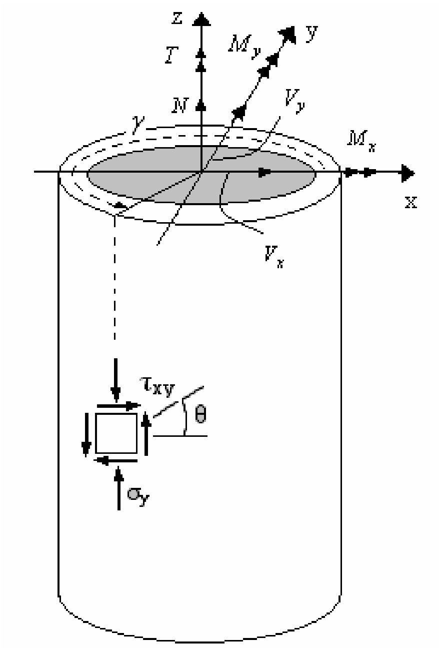

Figure 3. Loading acting at a medial cross section of a long bone.

The angle γ locate the angular position of the point of interest, at external bone surface, referred to *x* axis. The angle *θ* represents the orientation of the element of area (at figure *θ* = 0°) at external bone surface. Figure 4 shows the bending and transverse shear variables of a bi-material filled elliptic cross section of a long bone.

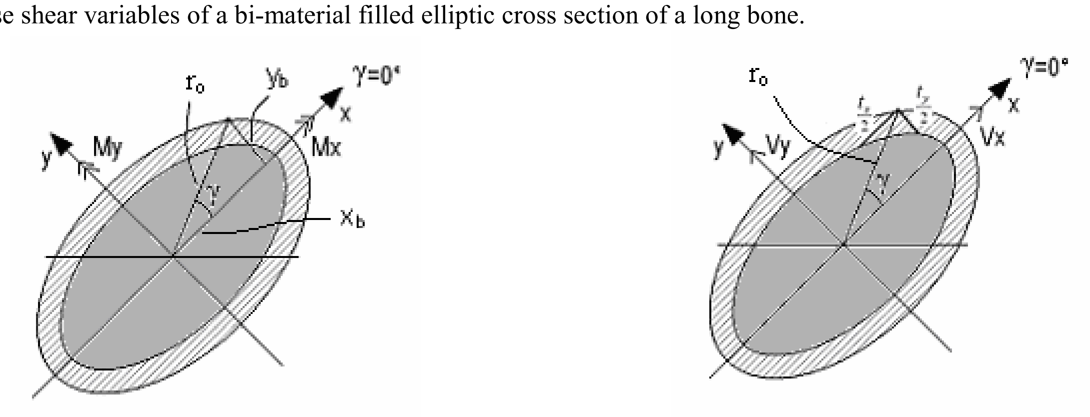

(a) (b)

Figure 4. Bi-material filled elliptic cross section: (a) Bending variables and (b) transverse shear variables.

The expressions of the analytic model will be presented in the following sequence: axial, bending, torsional and transverse shear stresses. The subscripts *C* and *T*, at the following expressions, means respectively cortical and trabecular bones.

The axial stress components, σ_{NC} and σ_{NT} are (Crandall, 1978):

$$\sigma_{NC} = \frac{N}{A_C + \frac{A_T}{n}} \quad \text{and} \quad \sigma_{NT} = \frac{N}{nA_C + A_T} \tag{4}$$

where, $A_C = \pi t\left(a+b-t\right)$ and $A_T = \pi\left(a-t\right)\left(b-t\right)$ (5)

$$n = \frac{E_C}{E_T} \tag{6}$$

Where E_C and E_T are, respectively, the modulus of elasticity of cortical and trabecular bones, *n* is the ratio between the two modulus of elasticity

The bending stresses components, σ_{BC_x} , σ_{BC_y} , σ_{BT_x} and σ_{BT_y} , are (Crandall, 1978):

$$\sigma_{BC_x} = \frac{y_b}{\left(1+\frac{1}{n\,m_x}\right)I_{C_x}} M_x \quad \text{and} \quad \sigma_{BC_y} = \frac{-x_b}{\left(1+\frac{1}{n\,m_y}\right)I_{C_y}} M_y \tag{7}$$

$$\sigma_{BT_x} = \frac{y_b}{\left(1+n\,m_x\right)I_{T_x}} M_x \quad \text{and} \quad \sigma_{BT_y} = \frac{-x_b}{\left(1+n\,m_y\right)I_{T_y}} M_y$$

$$x_b = r_o(\gamma)\cos(\gamma) \quad \text{and} \quad y_b = r_o(\gamma)\sin(\gamma) \quad \text{and} \quad r_o\left(\gamma\right) = \sqrt{a^2\cos^2(\gamma)+b^2\sin^2(\gamma)} \tag{8}$$

$$I_{C_x} = \frac{\pi}{4}\left[ab^3 - \left(a-t\right)\left(b-t\right)^3\right] \quad \text{and} \quad I_{C_y} = \frac{\pi}{4}\left[a^3 b - \left(a-t\right)^3\left(b-t\right)\right] \tag{9}$$

$$I_{T_x} = \frac{\pi}{4}\left[\left(a-t\right)\left(b-t\right)^3\right] \quad \text{and} \quad I_{T_y} = \frac{\pi}{4}\left[\left(a-t\right)^3\left(b-t\right)\right]$$

$$m_x = \frac{I_{Cx}}{I_{Tx}} \quad \text{and} \quad m_y = \frac{I_{Cy}}{I_{Ty}} \tag{10}$$

Where, x_b and y_b are respectively, the perpendicular distances from axis *y* and *x* to external bone surface. I_{C_x} , I_{C_y} , I_{T_x} and I_{T_y} are moments of inertia. *m* is the ratio between two moments of inertia, r_o is the external radius, the distance from the centre of cross section to the point of interest at external surface of bone.

Figure 5 shows a graphical representation of normal stress expressions (4)-(10). It shows a complete turn of angle γ at external surface of a medial section of a long bone. The geometric data were the same of a former work (Kenedi, 2009), based in (Bayraktar, 2004), (Bergmann, 2001) and (Rapoff, 2000), and the loading forces and moments were arbitrary chosen to maintain the stresses in an acceptable magnitude (Rudman, 2006).

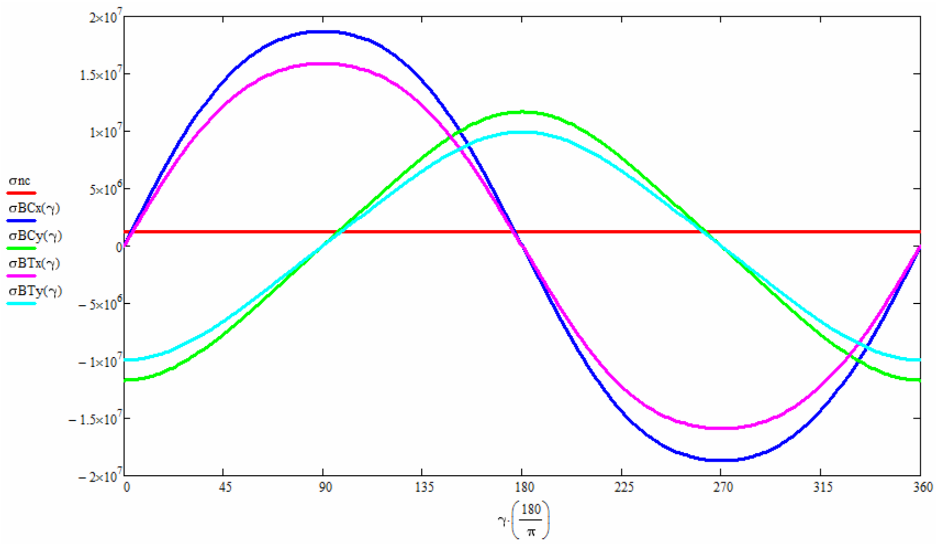

Figure 5. Axial and bending stresses components at external surface of a medial cross section of a long bone.

These curves show that axial stress is constant and bending stresses are maximum at the maximum distance of each neutral axis and null at each neutral axis.

The torsional stress τ_{TC} and τ_{TT} are (Crandall, 1978), (Patnaik,2004) and (Sadd, 2005):

$$\tau_{TC} = \frac{1}{2t\mathrm{A}} \frac{T}{\left(1+\dfrac{1}{p\,q}\right)} \quad \text{and} \quad \tau_{TT} = \frac{2}{\pi\,a\,b}\sqrt{\frac{x_b^2}{a^4}+\frac{y_b^2}{b^4}}\,\frac{T}{(1+p\,q)} \tag{11}$$

$$J_C = \frac{4\mathrm{A}^2 t}{\pi\left(a+b-t\right)} \quad \text{and} \quad J_T = \frac{\pi\,a\,b}{4}\left(a^2+b^2\right) \tag{12}$$

$$p = \frac{J_C}{J_T} \quad \text{and} \quad q = \frac{G_C}{G_T} \quad \text{and} \quad \mathrm{A} = \pi\left(a-\frac{t}{2}\right)\left(b-\frac{t}{2}\right) \tag{13}$$

Where, J_C and J_T are, respectively, the cortical and trabecular bone polar moments of inertia and G_C and G_T are, respectively, the cortical and trabecular bone shear modulus. A is the area inside a line which passes in middle thickness wall of cortical bone cross section. p is the ratio between two polar moment of inertia and q is the ratio between two shear modulus.

The transverse shear stress components, τ_{VC_x}, τ_{VC_y}, τ_{VT_x} and τ_{VT_y}, are (Crandall, 1978), (Patnaik,2004) and (Sadd, 2005):

$$\tau_{VCx} = \frac{Q_{yc}}{t_{yc}\left(1+\dfrac{1}{n\,m_y}\right)I_{Cy}}V_x \quad \text{and} \quad \tau_{VCy} = \frac{Q_{xc}}{t_{xc}\left(1+\dfrac{1}{n\,m_x}\right)I_{Cx}}V_y \tag{14}$$

$$\tau_{VTx} = \frac{Q_{yt}}{t_{yc}\left(1+n\,m_y\right)I_{Ty}}V_x \quad \text{and} \quad \tau_{VTy} = \frac{Q_{xt}}{t_{xc}\left(1+n\,m_x\right)I_{Tx}}V_y$$

where,

$$t_{xc} = 2a\sqrt{1-\left(\frac{y_b}{b}\right)^2} - \left[2(a-t)\sqrt{1-\left(\frac{y_b}{b-t}\right)^2}\right]k_x \quad \text{and} \quad t_{yc} = 2b\sqrt{1-\left(\frac{x_b}{a}\right)^2} - \left[2(b-t)\sqrt{1-\left(\frac{x_b}{a-t}\right)^2}\right]k_y \tag{15}$$

$$t_{xt} = 2\left(a-t\right)\sqrt{1-\left(\frac{y_b}{b-t}\right)^2} \quad \text{and} \quad t_{yt} = 2\left(b-t\right)\sqrt{1-\left(\frac{x_b}{a-t}\right)^2}$$

$$Q_{xc} = \int_{y_b}^{b} 2ay\sqrt{1-\left(\frac{y_b}{b}\right)^2}\,dy - \left[\int_{r_i(\gamma)\sin(\gamma)}^{b-t} 2(a-t)y\sqrt{1-\left(\frac{y_b}{b-t}\right)^2}\,dy\right]k_x \tag{16}$$

$$Q_{yc} = \int_{x_b}^{a} 2bx\sqrt{1-\left(\frac{x_b}{a}\right)^2}\,dx - \left[\int_{r_i(\gamma)\cos(\gamma)}^{a-t} 2(b-t)x\sqrt{1-\left(\frac{x_b}{a-t}\right)^2}\,dx\right]k_y$$

$$Q_{xt} = \int_{r_i(\gamma)\sin(\gamma)}^{b-t} 2(a-t)y\sqrt{1-\left(\frac{y_b}{b-t}\right)^2}\,dy \quad \text{and} \quad Q_{yt} = \int_{r_i(\gamma)\cos(\gamma)}^{a-t} 2(b-t)y\sqrt{1-\left(\frac{x_b}{a-t}\right)^2}\,dx \tag{17}$$

$$r_i\left(\gamma\right) = \sqrt{(a-t)^2\cos^2(\gamma)+(b-t)^2\sin^2(\gamma)} \tag{18}$$

Where, Q_{xc}, Q_{yc}, Q_{xt} and Q_{yt} are first moments of area, t_{xc}, t_{yc}, t_{xt} and t_{yt} are thicknesses. Note that $k_x = 0$ for $\left|y_b\right| \geq \left(b-t\right)$, $k_x = 1$ otherwise, and $k_y = 0$ for $\left|x_b\right| \geq \left(a-t\right)$, $k_y = 1$ otherwise.

Figure 6 shows a graphical representation of shear stress expressions (08) and (11)-(18). It shows a complete turn of angle γ at external surface of a medial long bone section. As was done at Fig.5, the geometric data were the same of a former work (Kenedi, 2009), based in (Bayraktar, 2004), (Bergmann, 2001) and (Rapoff, 2000), and the loading forces and moments were arbitrary chosen to maintain the stresses in an acceptable magnitude (Rudman, 2006).

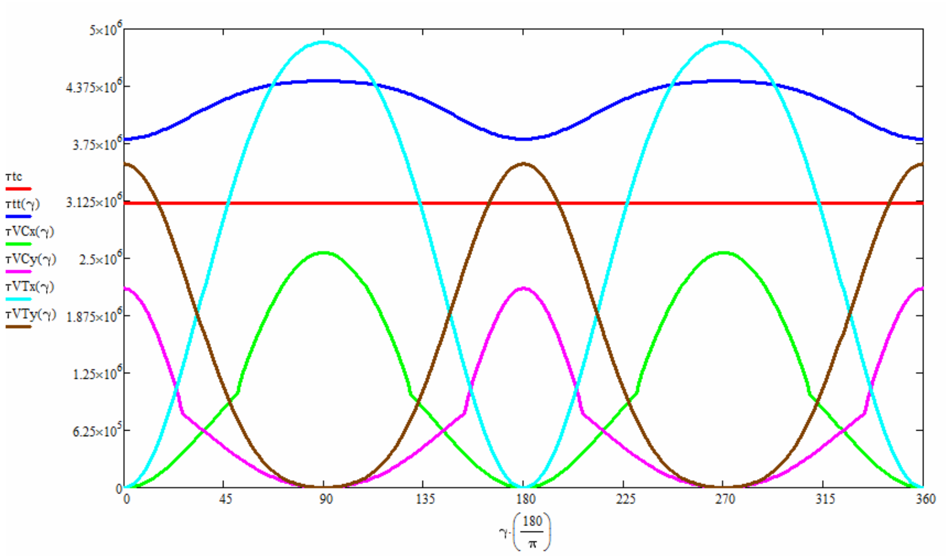

Figure 6. Torsional and transverse shear stresses components at external surface of a medial cross section of a long bone.

These curves show the torsional and transverse shear stress variation with the angular position γ. It is interesting to see the variation of transverse shear at cortical bone when passes from solid to hollow cross section.

2.3 – Mohr Circle

Using Mohr circle approach is possible to transform the axial, bending, torsional and transverse shear stresses in principal and maximum shear stresses. The resultant normal stress and the resultant shear stress can be estimated as shown at (20) and (21) expressions:

$$\sigma_y = \sigma_{NC} + \sigma_{BC} \text{ and } \tau_{xy} = \tau_{TC} + \tau_{VC} \qquad (20)$$

where, $\sigma_{BC} = \sigma_{BC_x} + \sigma_{BC_y}$ and $\tau_{VC} = \tau_{VC_x} + \tau_{VC_y}$. (21)

The principal stresses and angles at surface of a medial section of a long bone are:

$$\sigma_1, \sigma_3 = \frac{\sigma_y}{2} \pm \sqrt{\left(\frac{\sigma_y}{2}\right)^2 + \tau_{xy}^2} \quad , \quad \theta = \frac{1}{2}\arctan\left(\left|\frac{2\tau_{xy}}{\sigma_y}\right|\right) \qquad (22)$$

The maximum shear stress and angles at surface of a medial section of a long bone are:

$$\tau_{\max} = \sqrt{\left(\frac{\sigma_y}{2}\right)^2 + \tau_{xy}^2} \quad , \quad \theta' = \theta + 45^\circ \; or \; \theta' = \theta + 135^\circ \qquad (23)$$

3. CONCLUSIONS

A simple analytic model was developed, with limiting hypothesis, to describe the distribution normal and shear stresses componentes at external surface of a human medial long bone section, submitted to a static loading. The performance of analytic model was improved, in comparision with former work, by the utilization of two bones materials to model the cross section of a medial long bone. The possibility of estimatimation of principal and maximum shear stresses at external surface of medial long bone section, without the necessity of the utilization of a Finite Element Software, is the major goal of this work.

4. REFERENCES

Bayraktar, H.H. et al., (2004), "Comparison of the elastic and yield properties of human femoral trabecular and cortical bone tissue", J. Biomech., Vol. 37, pp. 27-35.

Bergmann, G. et al., (2001), "Hip contact forces and gait patterns from routine activities", J. Biomech., Vol. 34, pp.859-871.

Crandall, S.H., Dahl, N. C. and Lardner, T. J., (1978), "An Introduction to the Mechanics of Solids", Second Edition with SI units, Mc Graw Hill International Editions.

Doblaré, M., García J. M. and Gómez, M. J., (2004), "Modeling bone tissue fracture and healing: a review", Engineering Fracture Mechanics, Vol. 71, pp. 1809-1840.

Kenedi, P.P., Riagusoff, I.I.T., (2009b), "Stress Analysis Models of Human Long Bones – Analytic and Finite Analysis Approaches", In: Proceedings of 20th International Congress of Mechanical Engineering - COBEM 2009, Gramado, Rio Grande do Sul, 10-15 Nov.

Kenedi, P.P., Riagusoff, I.I.T., (2009a), "Analytic and finite element models of a human long bone", In: Anais do 2° Encontro Nacional de Engenharia Biomecânica, ENEBI 2009, Florianópolis, Santa Catarina, 6-8 Mai.

Kenedi, P.P., Riagusoff, I.I.T., (2008), "A Model of Stress Analysis of a Human Long Bone", In: Anais do 21º Congresso Brasileiro de Engenharia Biomédica, CBEB 2008, Salvador, Bahia, 16-20 Nov.

Kenedi, P.P., Riagusoff, I.I.T., (2007b), "A Comparative Analysis of Failures Criteria Applied to Long Bones", In: Proceedings of 19th COBEM, Brasilia, 5-9 Nov.

Kenedi, P.P., Riagusoff, I.I.T., (2007a), "Modeling initial fracture patterns in human long bones", In: Anais do 1° Encontro Nacional de Engenharia Biomecânica, ENEBI 2007, Petrópolis, Rio de Janeiro, 23-25 Mai.

Keyak, J. H., Rosi, S.A., (2000), "Prediction of femoral fracture load using finite element models: an examination of stress – and strain-based failure theories", J. Biomech., Vol. 33, pp. 209-214.

Patnaik, S. and Hopkins, D., (2004), "Strength of Materials: A Unified Theory", Elsevier.

Rapoff, A.J., (2007), "http://engineering.union.edu/~rapoffa/MER440/MER440.htm"

Rudman, K.E. et al., (2006), "Compression or tension? The stress distribution in the proximal femur", Biomedical Engineering Online, vol.5, No.12.

Sadd, M.H., (2005), "Elasticity – Theory, Applications and Numerics", Elsevier.

Turner, C.H. et al., (1999), "The elastic properties of trabecular and cortical bone tissues are similar: results from two microscopic measurement techniques", J. Biomech., Vol. 32, Technical Note, pp. 437-441.

5. RESPONSIBILITY NOTICE

The authors are the only responsible for the printed material included in this paper.